Rational Design of a Protein Kinase A Nuclear-cytosol Translocation Reporter

Allen K. Kim[1,2,3*], Takanari Inoue[1,2,3*]

[1]Department of Biomedical Engineering, Johns Hopkins University, School of Medicine, Baltimore, Maryland, United States.

[2]Department of Cell Biology, Johns Hopkins University, School of Medicine, Baltimore, Maryland, United States.

[3]Center for Cell Dynamics, Johns Hopkins University, School of Medicine, Baltimore, Maryland, United States.

[*]Correspondence to akim85@jhmi.edu, jctinoue@jhmi.edu

Abstract

Protein Kinase A (PKA) exists as a tetrameric holoenzyme which activates with increase of cAMP and plays an important role in many physiological processes including cardiac physiology, neuronal development, and adipocyte function. Although this kinase has been the subject of numerous biosensor designs, a single-fluorophore reporter that performs comparably to a Förster resonance energy transfer (FRET) has yet been reported. Here, we have used basic observations of electrostatic interactions in PKA substrate recognition mechanism and nucleus localization sequence motif to design a phosphorylation switch that shuttles between the cytosol and the nucleus, a strategy that should be generalizable to all basophilic kinases. The resulting reporter yielded comparable kinetics and dynamic range to the PKA FRET reporter, AKAR3EV. We also performed basic characterization and demonstrated its potential use in monitoring multiple signaling molecules inside cells using basic fluorescence microscopy. Due to the single-fluorophore nature of this reporter, we envision that this could find broad applications in studies involving single cell analysis of PKA activity.

Introduction

As one of the earlier kinases to be characterized, Protein Kinase A (PKA) has been discovered to play an important role in numerous physiological processes including cardiac physiology[1], neuronal development[2], and adipocyte function[3]. The kinase, in its inactive form, exists as a holoenzyme composed of two catalytic subunits and two regulatory subunits. Activation of the kinase is generally understood to occur through the increase of cAMP, which leads to the dissociation of the holoenzyme. Kinase activity can further be spatially regulated through the existence of A-kinase anchoring proteins which anchor the holoenzyme to specific subcellular localizations[4].

This well-characterized nature of PKA has naturally lent to it being used as a platform for number of interesting concepts for kinase reporters. One of the earliest of such designs was the utilization of Förster resonance energy transfer (FRET) to monitor the dissociation of the catalytic and regulatory subunits of the protein, a basic design that was used to demonstrate the localness of cAMP concentration and PKA activity[5]. A more generalizable variant of this design was established by Zhang, et al. which involved creating a chimera that consisted of FRET-compatible fluorescent proteins, a phosphopeptide binding domain, and a short kinase substrate sequence[6]. Upon phosphorylation, the binding affinity between the phosphopeptide binding domain and the substrate sequence dramatically increase leading to a conformational change, which is then measured through changes in FRET. This design has been the basis for number of generations of PKA FRET reporters existing in literature[7–11].

One of the main advantages of fluorescent kinase reporters is the ability to analyze kinase activity on a single cell level in real time. Despite this advantage, FRET reporters have the inherent downside of requiring two fluorophores, limiting the ability to monitor multiple kinases simultaneously with most experimental setups. Numerous groups have reported various approaches to overcome this limitation in

respect to PKA. These approaches have included using multiple FRET pairs[12], utilizing polarization of light as a readout[13], or designing proteins that changes subcellular localization in response to phosphorylation[14].

Our approach here utilizes a similar principle that we reported in a previous study where we designed a membrane-bound phosphorylation switch[15]. In summary, arginines in the P-2 and P-3 positions are important residues for substrate recognition[16,17]. By placing the amino acid sequence for the substrate in tandem with minor modifications, we designed an amino acid sequence that loosely conformed to known consensus nuclear localization sequence (NLS) motifs[18]. This peptide responded to PKA activity by shuttling between the nucleus and the cytosol. We furthermore performed basic optimization and demonstrated its use in simultaneously monitoring two different signals within a cell.

Methods

Cell Culture and Transfection

HeLa cells were cultured in DMEM with 10% FBS and routinely passaged. Cells were seeded at a density of 2.0×10^4 cells/cm^2 in a 6-well plate containing a 25 mm coverslip one day before transfection. They were transfected with multiple plasmids at an amount of 50 ng each using FugeneHD according to manufacturer's protocol. On the following day, culture media was replaced with serum-free DMEM in the morning. Imaging took place in the afternoon of the same day.

Image Acquisition

Images were acquired on an inverted microscope (IX81, Olympus) with a heated incubator that maintained the chamber at 37° and 5% CO_2 (WELS, Tokai-Hit). Images were acquired for either 15 or 25 minutes at 1-minute interval. Drugs were added at the 5-minute and 15-minute point. PKA activation was achieved through treatment with 50 µM forskolin and 100 µM IBMX, unless otherwise noted. For the experiment demonstrating reversibility, the media was replaced with new media containing 40 µM H89

at the 15-minute point, as residual forskolin and IBMX led to an incomplete inhibition of PKA. Images were acquired with a CMOS camera (C11440, Hamamatsu) in a 60x oil objective (Plan Apo N, Olympus) with the appropriate excitation and emission filters driven by a filter wheel controller. Metamorph was used to control the hardware associated with the microscope which includes the motorized stage (MS-2000, Applied Scientific Instrumentation), filter wheels (Lambda 10-3, Sutter Instruments), and LED light source (pE-300, CoolLED). To measure response with the FRET reporter, cells were excited on the CFP channel, and images were acquired on the YFP channel.

Image Analysis

All cells were co-transfected with H2B-mCherry (Figs 1, 2, 3, S1) or H2B-mCerulean3 (Figs 4, S2) to mark the nucleus. Using the H2B as a mask, ImageJ was used to distinguish cytosolic fluorescent signal from the nuclear signal. The fluorescent signal change was tracked by creating a ratio of cytosol-to-nuclear signal. For FRET experiments, the fluorescent signal was tracked by tracking the ratio from YFP emission to CFP emission. For response profiles, data was normalized by the average of the pre-treatment signals. For all experiments excluding the experiment involving duplex monitoring, analysis was carried out across 3 independent experiments. 10 cells were analyzed from each experiment, resulting in a total of 30 cells analyzed. Student's t-test for unequal variance was used to test for statistical significance in Figs 2D and 3D.

DNA Cloning

The cDNA for H2B (gift from Sergi Regot) was amplified by PCR and inserted into NheI and AgeI site of the mCherry-C1 and mCerulean3-C1 vectors (Clontech). YFP-PH(Akt) is a standard PH domain construct for PIP_3 labeling. All the reporter variants were inserted into the EYFP-C1 vector (Clontech) at the SacII and BamHI restriction sites using annealed oligonucleotides. The forward sequences of the annealed oligonucleotides are tabulated below:

DNA construct	cDNA sequence	Amino acid sequence
Substrate	GGGCctgagaagagccagcctgggcTAGG	LRRASLG
Substrate$_2$	GGGCctgagaagagccagcctgggcaagagaaga gccagcctgggcTAGG	LRRASLGKRRASLG
Substrate$_3$	GGGCctgagaagagccagcctgggcaagagaaga gccagcctgggcaagagaagagccagcctgggcTA GG	LRRASLGKRRASLGKRRASLG
Substrate$_4$	GGGCctgagaagagccagcctgggcaagagaaga gccagcctgggcaagagaagagccagcctgggcaag agaagagccagcctgggcTAGG	LRRASLGKRRASLGKRRASLGKRRASLG
Substrate$_3$-NesA	GGGCctgagaagagccagcctgggcaagagaaga gccagcctgggcaagagaagagccagcctgggcgtg gaccagctgagactggagagactgcagatcgacgag TAGG	LRRASLGKRRASLGKRRASLGVDQLRL ERLQIDE
Substrate$_3$(AAA)-NesA	GGGCctgagaagagccgccctgggcaagagaaga gccgccctgggcaagagaagagccgccctgggcgtg gaccagctgagactggagagactgcagatcgacgag TAGG	LRRAALGKRRAALGKRRAALGVDQLRL ERLQIDE
Substrate$_3$-NesB	GGGCctgagaagagccagcctgggcaagagaaga gccagcctgggcaagagaagagccagcctgggcgac cccctgcccgtgctggagaacctgaccctgaagagcT AGG	LRRASLGKRRASLGKRRASLGDPLPVLE NLTLKS
Substrate$_3$-NesC	GGGCctgagaagagccagcctgggcaagagaaga gccagcctgggcaagagaagagccagcctgggcaag gtggccgagaagctggaggccctgagcgtgaaggag TAGG	LRRASLGKRRASLGKRRASLGKVAEKLE ALSVKE
Substrate$_3$-NesD	GGGCctgagaagagccagcctgggcaagagaaga gccagcctgggcaagagaagagccagcctgggcgcc ctgcagaagaagctggaggagctggagctggacgag TAGG	LRRASLGKRRASLGKRRASLGALQKKLE ELELDE

Results

We designed a phosphorylation switch based on the basic observation that the PKA substrate can be arranged in tandem to form a NLS. Due to the overlapping nature of the NLS with the phosphate acceptor, phosphorylation of this peptide results in a shift in localization. Our final design consisted of NLS and nuclear export sequence (NES), where the NLS contained the three phosphate acceptors for PKA (Fig 1A).

When the reporter was fused to EYFP and transfected in cells, this peptide responded to PKA activation by 50 µM forskolin and 100 µM IBMX by redistributing from the nucleus to the cytosol (Fig 1B). When the signal change was quantified by taking the ratio of cytosolic fluorescence signal to nuclear signal, the

kinetics and dynamic range was comparable to the FRET reporter, AKAR3EV[9]. The response to 40 µM H89, which resulted in the inhibition of PKA, also revealed a similar kinetics and response to its FRET counterpart. A serine-to-alanine mutation of all the phosphate acceptors led to no response, while removing the NES led to a much slower response to the activation. Representative images show the change in localization of the EFYP within the 3 minutes following PKA activation (Fig 1C).

To reach the final design, we first designed a switchable NLS. We utilized the Kemptide (LRRASLG)[16], a well-established PKA substrate, as the working unit of the design, which contains the two arginines in the P-2 and P-3 position considered important for substrate recognition. A monovalent substrate alone does not conform to known NLS. However, placing these sequences in tandem leads to a sequence that conforms loosely to NLS motif (Fig 2A). We transfected cells with EYFP fused to various number of substrates. Increasing the number of substrates led to a concomitant increase in nuclear localization (Fig 2B). When cells were treated with forskolin and IBMX, the fluorescent signal redistributed to become more diffuse at the end of 10 minutes of treatment determined by a normalized response profile (Fig 2C). The pre-treatment localization and the post-treatment localizations was determined by measuring the ratio of cytosol-to-nuclear fluorescent signal (Fig 2D). We also tested a construct containing four substrates. However, because of the strong nuclear localization, there was very little measurable cytosolic signal. For this peptide, we measured the depletion of nuclear signal and observed little difference compared to the construct containing three substrates (Fig S1). Given these considerations, the trivalent form was considered optimal. However, the response kinetics of the peptide was substantially slower than its counterpart FRET reporter (Fig 1B, blue).

To mitigate this difference in response kinetics, we fused a NES to the trivalent substrate. A previous study established the relative strengths of the various NES's[19]. Using this as a reference, we fused a 13-amino-acid, leucine-rich fragment from FMR1, TFIIIA, RanBP1, and Map2K1 (Fig 3A). We observed that three of the four NES's overpowered the NLS (Fig 3B). This also translated to a decrease in both response amplitude

and kinetics (Figs 3C, 3D). Amongst the four sequences tested, the NES fragment from FMR1 protein led to a substantial improvement in kinetics and dynamic range in comparison to the peptide lacking a NES. The kinetics and response of this design was comparable to that observed with the FRET reporter (Fig 1B, blue).

Lastly, by co-transfecting the PH domain from Akt (mCherry) and the PKA phosphorylation switch (EYFP), we simultaneously monitored the synthesis of PIP_3, a lipid secondary messenger, and the activity of PKA. Upon stimulation with 50 ng/mL EGF, we observed a transient increase in PIP_3, indicated by the translocation of the PH domain from the cytosol to the plasma membrane (Fig 4A). This was indicated by the accumulation of PH domain at the plasma membrane upon activation with EGF but not upon PKA activation (Fig 4B). PKA activity as measured by the reporter led to a sustained level of increase upon activation of EGF and saturated with treatment of the forskolin and IBMX cocktail (Fig 4C). We also reversed the order of treatment and observed PIP_3 enrichment only when the cells were treated with EGF (Fig S2).

Discussion

Our PKA phosphorylation switch is *de novo* amino acid sequence based on simple observations of PKA consensus sequence and NLS motif. Using this information, we designed a switch that reproduced the kinetics measured with a well-established FRET reporter. In contrast to FRET reporters, this type of single-fluorophore reporter frees up a fluorescent color, allowing for an additional channel of analysis. We then demonstrated this capability monitoring two different signaling molecules by overexpressing cells with the PH domain from Akt and the PKA reporter.

A switchable NLS alone did not reproduce the kinetics of PKA activation observed with a FRET reporter. The distribution of a protein observed in a cell is determined by the net flux of the nuclear import and nuclear export transport processes. With peptides containing only NLS's, the nuclear import is driven by

facilitated diffusion while nuclear export is driven by passive diffusion. As passive diffusion is slower than facilitated diffusion, the time required to reach steady state is longer, reflected by the decrease in response kinetics. The addition of a NES mitigated this issue. An ideal reporter, thus, should be rate-limited by the kinetics of the underlying phosphorylation not by auxiliary processes.

Another important property of reporters is kinase specificity. In our study, we have used a well-characterized substrate sequence of PKA that has been used in previous FRET reporters[7–11]. Phosphorylation prediction algorithm, NetPhos3.1[20], strongly suggests PKA as the target kinase for this reporter. Furthermore, based on current literature of AGC kinases, PKA is the only AGC kinase that requires two arginines at P-2 and P-3 position[16,17,21,22]. These reports do not rigorously rule out non-specific phosphorylation, as substrates are not necessarily required to conform to consensus sequences. However, given current literature and our data, PKA activity appears to be the driving force behind the shuttling.

We used the interaction of positively charged residues in the substrate sequence to the catalytic subunit of PKA to design the reporter. However, this is not necessarily the only method of achieving specificity. Regot, et al. developed a similar reporter which shuttles between the cytosol and the nucleus using a different strategy[14]. The phosphate acceptors in this reporter are placed in a much weaker, proline-rich substrate recognition sequence derived from c-Jun. The affinity towards the substrate is increased through docking sequences, which elevates the effective concentration of the substrate to the kinase[23,24]. We were unable to observe a measurable response with this PKA reporter. However, we speculate that this reporter design relies on a much weaker interaction with the kinase than our design, requiring a more careful optimization of experimental conditions.

In summary, we have designed a reporter based on a rearrangement of a PKA substrate to create a NLS. In principle, this is generalizable to all basophilic kinases, as this mechanistically relies on disruption of electrostatic interactions through phosphorylation. Due to the single-fluorophore nature of this reporter

and its comparable performance to a FRET reporter, we envision that this could find broad applications in studies involving single cell analysis of PKA activity.

Acknowledgments

We would like to thank Dr. Kazuhiro Aoki for providing the AKAR3EV construct. This study was supported by National Institute of Health R01 GM123130 and DARPA HR0011-16-C-0139 (to T.I.).

Author Contributions

T.I. and A.K.K. conceived and designed this study. A.K.K. conducted all experiments and analyses. A.K.K. wrote the manuscript with contributions from T.I.

References

1. Perera, R. K. & Nikolaev, V. O. Compartmentation of cAMP signalling in cardiomyocytes in health and disease. *Acta Physiol.* **207**, 650–662 (2013).
2. Park, H. & Poo, M. Neurotrophin regulation of neural circuit development and function. *Nat. Rev. Neurosci.* **14**, 7–23 (2013).
3. Sethi, J. K. & Vidal-Puig, A. J. *Thematic review series: Adipocyte Biology.* Adipose tissue function and plasticity orchestrate nutritional adaptation. *J. Lipid Res.* **48**, 1253–1262 (2007).
4. Wong, W. & Scott, J. D. AKAP signalling complexes: focal points in space and time. *Nat. Rev. Mol. Cell Biol.* **5**, 959–970 (2004).
5. Zaccolo, M. Discrete Microdomains with High Concentration of cAMP in Stimulated Rat Neonatal Cardiac Myocytes. *Science* **295**, 1711–1715 (2002).
6. Zhang, J., Ma, Y., Taylor, S. S. & Tsien, R. Y. Genetically encoded reporters of protein kinase A activity reveal impact of substrate tethering. *Proc. Natl. Acad. Sci.* **98**, 14997–15002 (2001).
7. Zhang, J., Hupfeld, C. J., Taylor, S. S., Olefsky, J. M. & Tsien, R. Y. Insulin disrupts β-adrenergic signalling to protein kinase A in adipocytes. *Nature* **437**, 569–573 (2005).
8. Allen, M. D. & Zhang, J. Subcellular dynamics of protein kinase A activity visualized by FRET-based reporters. *Biochem. Biophys. Res. Commun.* **348**, 716–721 (2006).
9. Komatsu, N. *et al.* Development of an optimized backbone of FRET biosensors for kinases and GTPases. *Mol. Biol. Cell* **22**, 4647–4656 (2011).
10. Depry, C., Allen, M. D. & Zhang, J. Visualization of PKA activity in plasma membrane microdomains. *Mol BioSyst* **7**, 52–58 (2011).
11. Tillo, S. E. *et al.* Liberated PKA Catalytic Subunits Associate with the Membrane via Myristoylation to Preferentially Phosphorylate Membrane Substrates. *Cell Rep.* **19**, 617–629 (2017).
12. Aye-Han, N.-N., Allen, M. D., Ni, Q. & Zhang, J. Parallel tracking of cAMP and PKA signaling dynamics in living cells with FRET-based fluorescent biosensors. *Mol. Biosyst.* **8**, 1435 (2012).
13. Ross, B. L. *et al.* Single-color, ratiometric biosensors for detecting signaling activities in live cells. *eLife* **7**, (2018).

14. Regot, S., Hughey, J. J., Bajar, B. T., Carrasco, S. & Covert, M. W. High-Sensitivity Measurements of Multiple Kinase Activities in Live Single Cells. *Cell* **157**, 1724–1734 (2014).
15. Kim, A. K. & Inoue, T. Rational design of a synthetic farnesyl-electrostatic switch based on the hypervariable region of K-Ras4b. *bioRxiv* (2019). doi:10.1101/635839
16. Kemp, B. E., Graves, D. J., Benjamini, E. & Krebs, E. G. Role of multiple basic residues in determining the substrate specificity of cyclic AMP-dependent protein kinase. *J. Biol. Chem.* **252**, 4888–4894 (1977).
17. Hutti, J. E. *et al.* A rapid method for determining protein kinase phosphorylation specificity. *Nat. Methods* **1**, 27–29 (2004).
18. Kosugi, S. *et al.* Six Classes of Nuclear Localization Signals Specific to Different Binding Grooves of Importin α. *J. Biol. Chem.* **284**, 478–485 (2009).
19. Henderson, B. R. & Eleftheriou, A. A Comparison of the Activity, Sequence Specificity, and CRM1-Dependence of Different Nuclear Export Signals. *Exp. Cell Res.* **256**, 213–224 (2000).
20. Blom, N., Sicheritz-Pontén, T., Gupta, R., Gammeltoft, S. & Brunak, S. Prediction of post-translational glycosylation and phosphorylation of proteins from the amino acid sequence. *PROTEOMICS* **4**, 1633–1649 (2004).
21. Obata, T. *et al.* Peptide and Protein Library Screening Defines Optimal Substrate Motifs for AKT/PKB. *J. Biol. Chem.* **275**, 36108–36115 (2000).
22. Nishikawa, K., Toker, A., Johannes, F.-J., Songyang, Z. & Cantley, L. C. Determination of the Specific Substrate Sequence Motifs of Protein Kinase C Isozymes. *J. Biol. Chem.* **272**, 952–960 (1997).
23. Kallunki, T., Deng, T., Hibi, M. & Karin, M. c-Jun Can Recruit JNK to Phosphorylate Dimerization Partners via Specific Docking Interactions. *Cell* **87**, 929–939 (1996).
24. Ubersax, J. A. & Ferrell Jr, J. E. Mechanisms of specificity in protein phosphorylation. *Nat. Rev. Mol. Cell Biol.* **8**, 530–541 (2007).

Figure 1: Basic design of the PKA kinase reporter.

(A) Design consists of a NLS with three phosphorylation sites fused to a NES sequence. Phosphorylation regulates the activity of the NLS. Basic residues are colored blue; phosphoserine is colored red; and NES is colored green.

(B) Response profile shows the normalized signal change resulting from the activation and inhibition of PKA FRET reporter (blue) and three variants of the nuclear-cytosol translocation reporter. The three variants are: a full version with the NES (yellow), a version lacking the NES (green), and a full version with serine-to-alanine mutations (red).

(C) Representative images show the changes in distribution of the full version of the reporter that occurs within three minutes of PKA activation.

All data points in this figure represent an average signal intensity calculated from 30 cells over 3 independent experiments. Error bar represents standard error of mean. Scale bar represents 10 µm.

Figure 2: Effects of valency on initial localization and response to PKA activation.

(A) Representative images show the initial distribution (Pre) and the distribution 10 minutes post-treatment (Post) for peptides containing one, two, and three substrates.

(B) Response profile shows the normalized signal change resulting from the activation of PKA for peptide consisting of one (blue), two (yellow), and three (black) substrates.

(C) Bar chart represents the pre-treatment localization (blue) and post-treatment localization (red) as measured by taking the ratio of cytosol-to-nuclear fluorescent signal for peptide consisting of one, two, and three substrates.

(D) Table contains the amino acid sequences of the peptides containing the different number of substrates.

All data points in this figure represent an average signal intensity calculated from 30 cells over 3 independent experiments. Error bar represents standard error of mean. * represents $p<0.001$. Scale bar represents 10 µm.

Figure 3: Effects of addition of NES on initial localization and response to PKA activation.

(A) Representative images show the initial distribution (Pre) and the distribution 10 minutes post-treatment (Post) for peptides fused with NesA, NesB, NesC, and NesD.

(B) Response profile shows the normalized signal change resulting from the activation of PKA for peptide consisting fused with NesA (blue), NesB (yellow), NesC (green), and NesD (red) along with a peptide without NES (black).

(C) Bar chart represents the pre-treatment localization (blue) and post-treatment localization (red) as measured by taking the ratio of cytosol-to-nuclear fluorescent signal for peptides fused with NesA, NesB, NesC, and NesD compared to a peptide without NES.

(D) Table contains the amino acid sequences of the NES that was fused to the peptide along with the derived gene names.

All data points in this figure represent an average signal intensity calculated from 30 cells over 3 independent experiments. Error bar represents standard error of mean. * represents $p<0.001$. Scale bar represents 10 µm.

Figure 4: Duplex monitoring of PIP_3 and PKA in a single cell

(A) Representative images show PIP_3 accumulation (as indicated by translocation of PH domain) and PKA activity in a single cell after EGF treatment followed by PKA activation.

(B) Line-scan of the image in Figure 4A (white line) shows the transient appearance of enriched fluorescent signal at the plasma membrane (arrows).

(C) Response profile shows the normalized signal change that results from EGF stimulation followed by a saturation of the reporter response with forskolin and IBMX cocktail.

Data points represent measurement from a single cell. Scale bar represents 10 µm.

Figure S1: Response of tetravalent substrate to PKA activation.

(A) Representative images show the localization of YFP-Sub_4 pre-treatment (Pre) and 10 minutes post-treatment (Post).

(B) Response profile shows the normalized change in nuclear fluorescent signal after PKA activation with the peptides containing the different number of substrates.

All data points in this figure represent an average signal intensity calculated from 30 cells over 3 independent experiments. Error bar represents standard error of mean. Scale bar represents 10 µm.

Figure S2: Duplex monitoring of PIP_3 and PKA in a single cell with PKA activation followed by EGF treatment.

(A) Representative images show PKA activity and PIP_3 accumulation (as indicated by translocation of PH domain) in a single cell after PKA activation followed by EGF treatment.

(B) Line-scan of the image in Figure 4A (white line) shows the transient appearance of enriched fluorescent signal at the plasma membrane with EGF treatment but not with PKA activation (arrows).

(C) Response profile shows the normalized signal change that results from PKA activation followed by EGF stimulation.

Data points represent measurement from a single cell. Scale bar represents 10 µm.

Figure 1

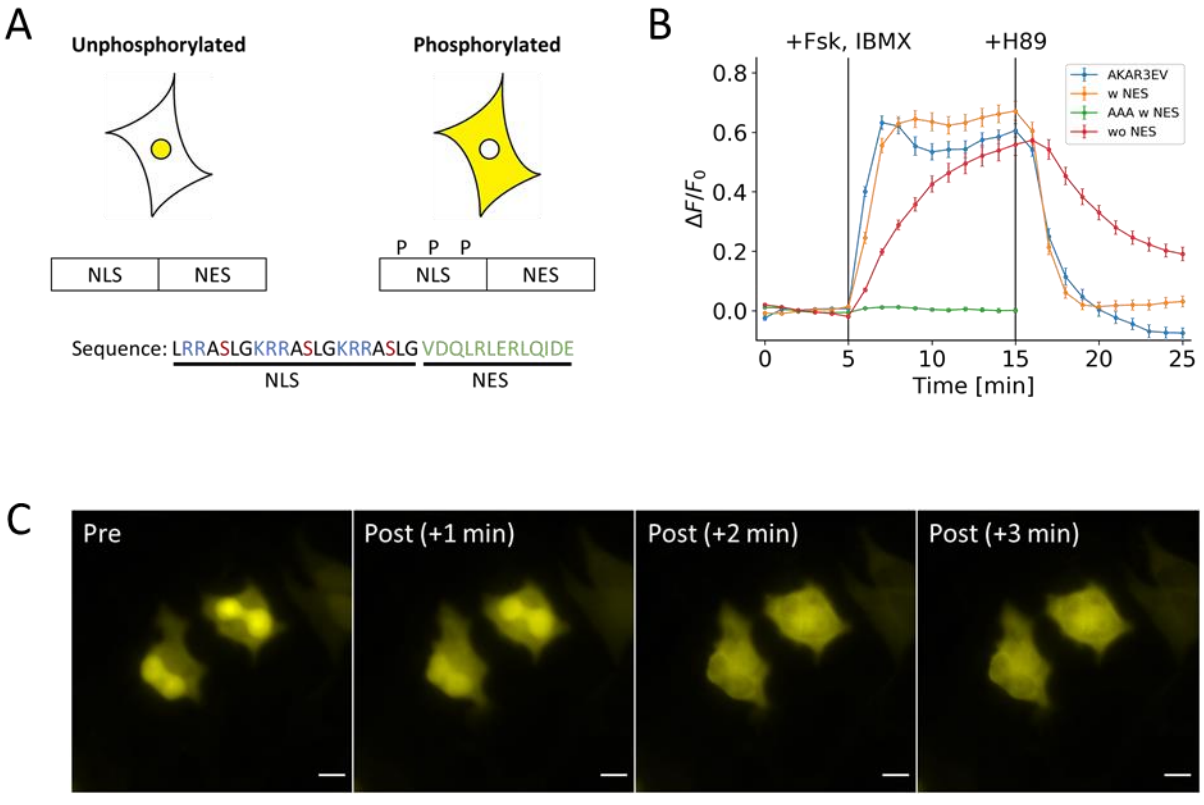

1 Figure 2

A

	Sequence
Sub_1	LRRASLG
Sub_2	LRRASLG-K-RRASLG
Sub_3	LRRASLG-K-RRASLG-K-RRASLG
Sub_4	LRRASLG-K-RRASLG-K-RRASLG-K-RRASLG

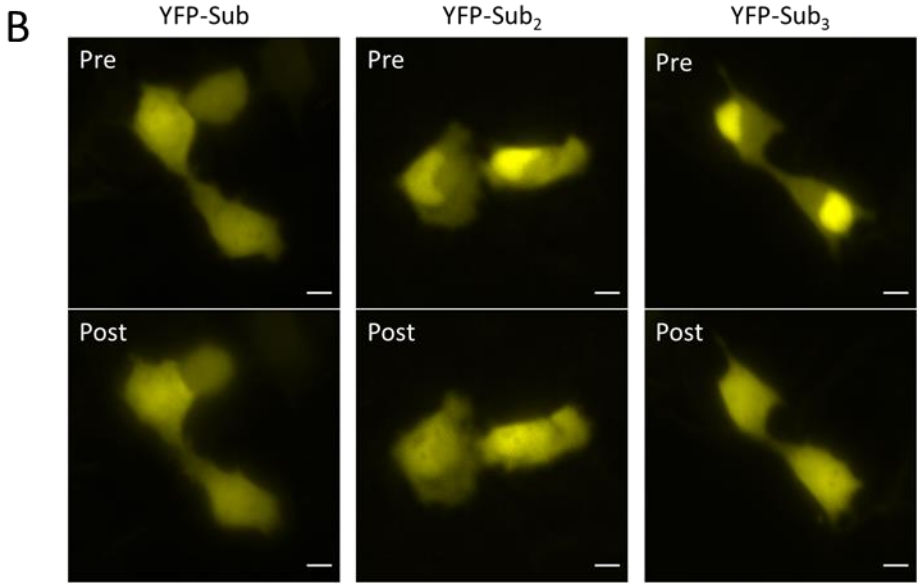

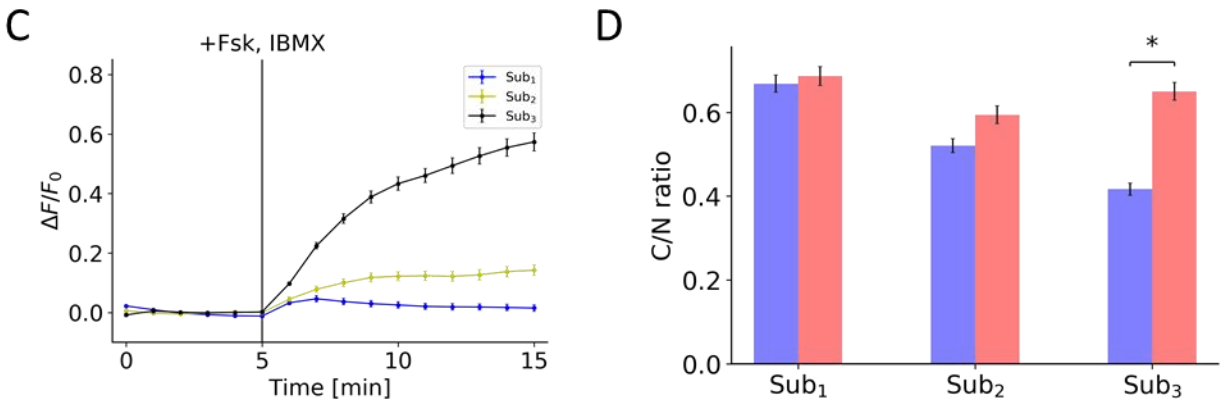

2

Figure 3

A

	Derived protein	Sequence
NesA	FMR1 (427-439)	VDQLRLERLQIDE
NesB	TFIIIA (328-339)	DPLPVLENLTLK*S
NesC	RANBP1 (179-191)	KVAEKLEALSVKE
NesD	MAP2K1 (32-44)	ALQKKLEELELDE

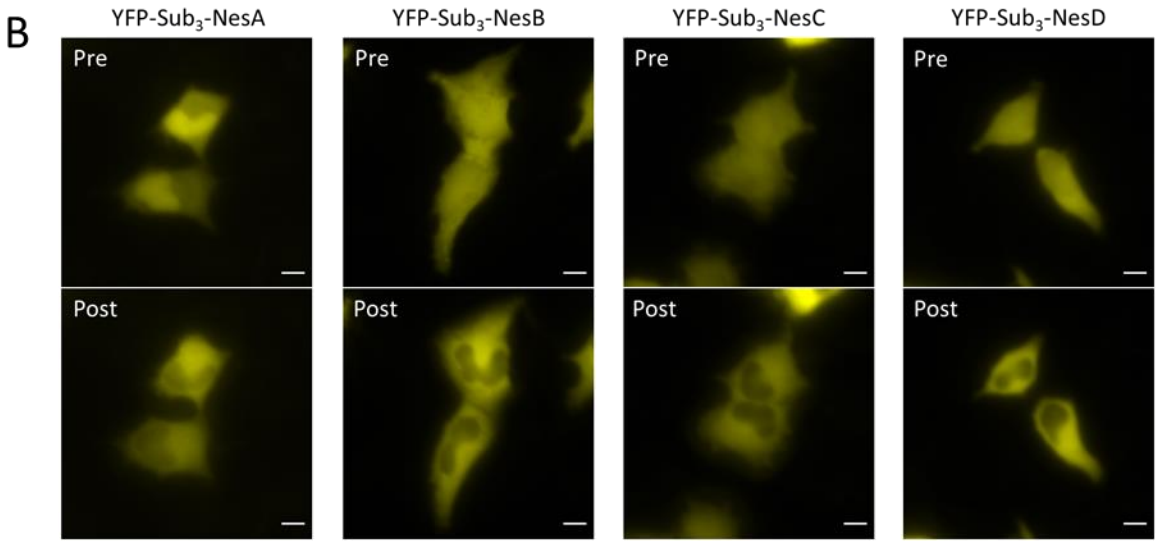

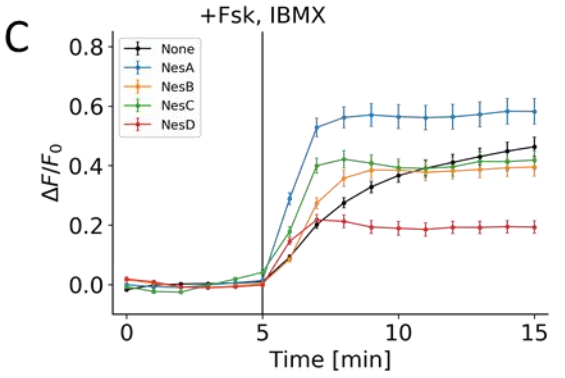

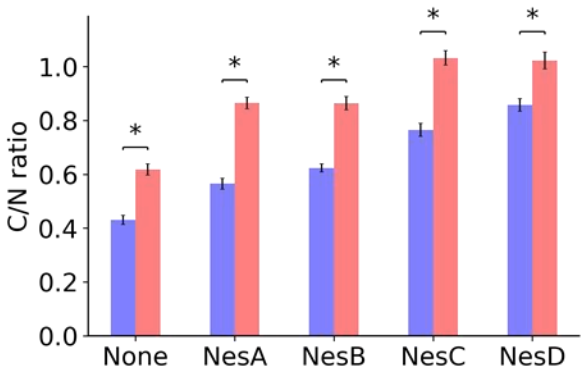

Figure 4

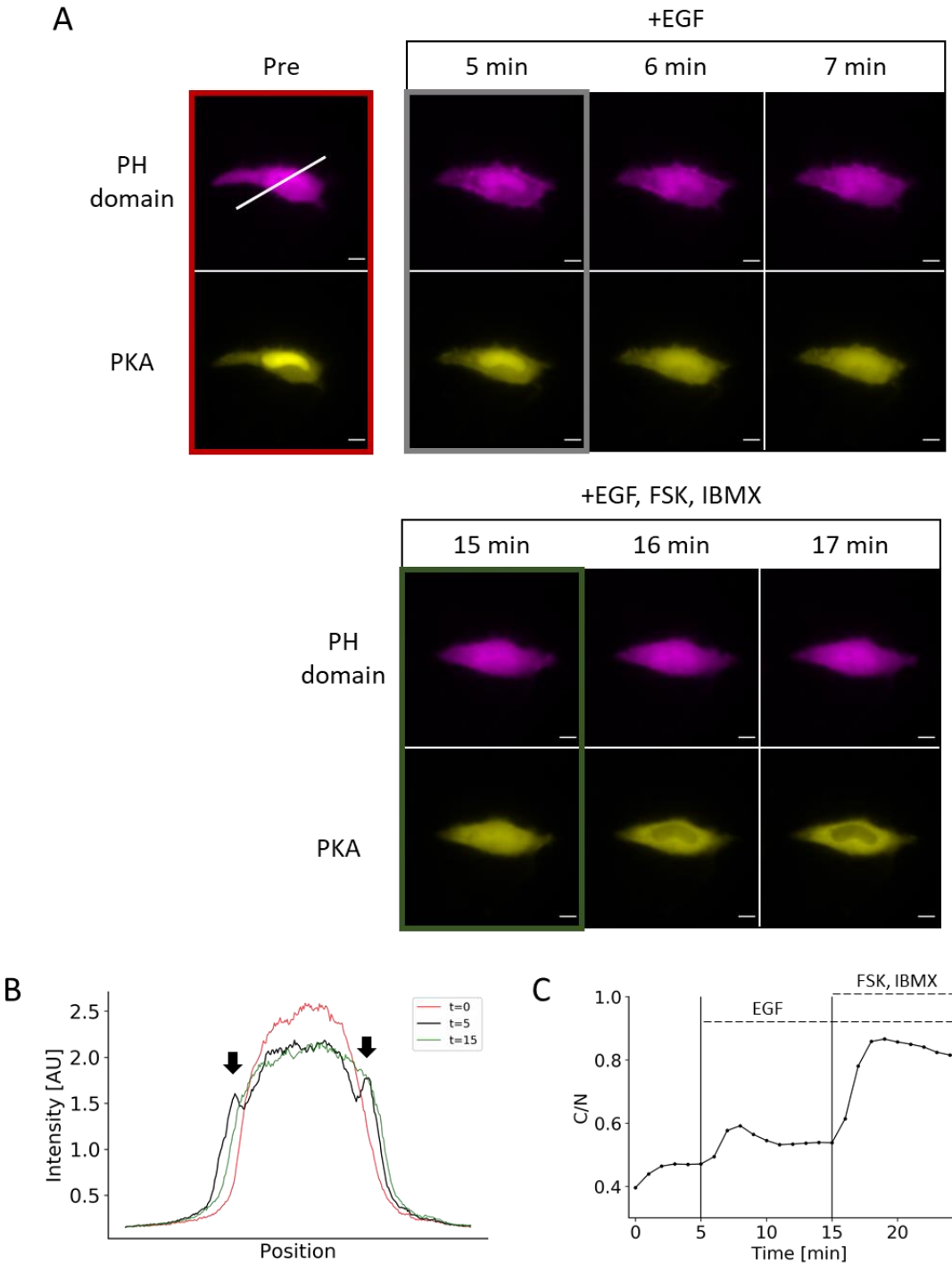

Figure S1

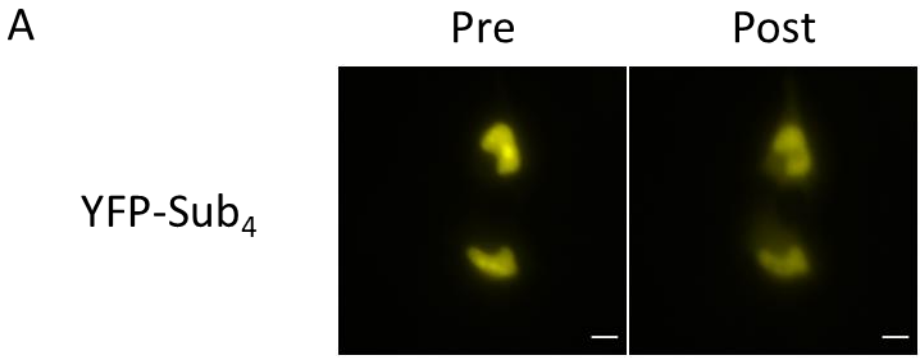

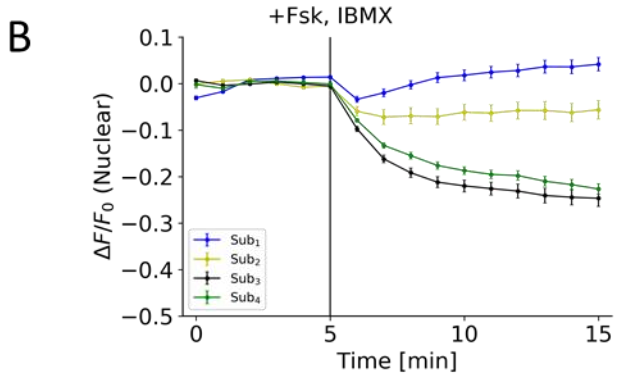

Figure S2